View metadata, citation and similar papers at core.ac.uk

brought to you by CORE

provided by DSpace@MIT

HHS Public Access

Author manuscript

Small. Author manuscript; available in PMC 2016 September 01.

Published in final edited form as:

Small. 2015 September ; 11(36): 4643–4650. doi:10.1002/smll.201500674.

Development of a High-Throughput Functional Screen using Nanowell-Assisted Cell Patterning

Ayca Yalcin Ozkumur[1,†], **Brittany A. Goods**[2,†], and **J. Christopher Love**[3,4,5,*]

[1]Electrical and Electronics Engineering Department, Bahcesehir University, Istanbul, Turkey

[2]Department of Biological Engineering, Koch Institute for Integrative Cancer Research at MIT, Cambridge, Massachusetts 02139, USA

[3]Department of Chemical Engineering, Koch Institute for Integrative Cancer Research at MIT Cambridge, Massachusetts 02139, USA

[4]The Broad Institute of MIT and Harvard, Cambridge, MA 02142, USA

[5]The Ragon Institute of MGH, MIT and Harvard, Cambridge, MA 02139, United States

Abstract

Assays used for high-throughput screening often rely on viable cells to facilitate lead discovery of functional therapeutics of interest, such as neutralizing antibodies. The reliance on living cells has traditionally constrained the form factor of these assays to common microtitre plates (e..g., 96-, 384-, 1536-well plates). This form factor can constrain the total numbers of unique assays performed (number of plates examined) in part due to the costs of media and components used. We sought to develop a simple and efficient format to implement functional assays for screening biological responses that rely on cell-based signal readouts. We report a versatile and scalable method that uses dense arrays of subnanoliter wells (nanowells) for imparting defined patterns on monolayers of cells. The living cell arrays produced by nanowell-assisted cell patterning (NWAP) can easily be assayed for migration, proliferation, viability and accumulation of reporter signal. We also show that this approach can coordinate a multi-component biological assay by designing and implementing a high-throughput, functional nanoliter-scale neutralization assay to identify neutralizing antibodies against HIV. The flexible assay format allows for the interrogation of thousands of individual antibody secreting cells in parallel, making it well-suited for screening libraries of cells producing candidate lead antibodies based on functions like neutralizing activity.

Keywords

cell patterning; living-cell arrays; neutralization; HIV

[*]Corresponding author at: Department of Chemical Engineering, Koch Institute for Integrative Cancer Research, Massachusetts Institute of Technology, 77 Massachusetts Ave., Bldg. 76-253, Cambridge, MA 02139, United States. Tel.: +1 617 324 2300. clove@mit.edu (J.C. Love).

[†]These authors contributed equally to this work.

Supporting Information

Supporting Information is available from the Wiley Online Library or from the author.

Author Manuscript

Author Manuscript

Author Manuscript

Author Manuscript

Author Manuscript Author Manuscript Author Manuscript Author Manuscript

Given the therapeutic promise of monoclonal antibodies, there is a need for efficient, functional, and scalable screens for identifying potent antibodies early in the development process.[1] For many antibodies, such as neutralizing antibodies or bi-specific antibodies for cancer therapy, binding alone does not imply functional activity. Thus, the use of biomolecular and biochemical assays alone is not sufficient for lead identification of functional therapeutics.[2]

The use of cell-based screening assays has facilitated the identification of therapeutically relevant biologics. For example, strongly neutralizing antibodies against human immunodeficiency virus (HIV), such as PG9 and PGT121,[3] have been successfully identified with these methods. Cell-based assays, such as virus neutralization or targeted killing assays, are valuable because they allow for molecular characterization in a biologically relevant context. The widespread utility of cell-based assays coupled with their potential for increasing success in discoveries of lead compounds necessitates the development of technologies that enable their implementation in high-throughput formats. In their current microtitre plate-based format, these assays have limited scalability and are not cost effective.[4]

One proposed solution to the low throughput of plate-based assays is to use droplet-based screens.[5,6] Microfluidics-based droplet screens have been successfully implemented to enrich for monoclonal antibodies based on binding[2] and for the optimization of chemical screens.[6] However, the complexity of designing microfluidic devices, and the inability to repeatedly track single droplets over time hinder the development of assays that require the study of time-dependent biological behavior, such as migration, neutralization, or cell-mediated killing.[7] Alternatively, living cell arrays, where cells are spatially patterned on a substrate, can provide controlled and high-throughput systems in which to study the effect of stimuli, such as a potential therapeutic, on long-term cell fate and phenotype.[8,9] Many methods have been developed for patterning cells on various substrates; these vary in their simplicity, ease-of-use, and versatility. In principal, each technique relies on creating patterns of materials that promote or resist adherence of cells. These materials can be patterned using many techniques, including microarray printing,[8] soft-lithography-based stamping or stenciling techniques,[10] layer-by-layer assembly,[11] microfluidics,[12] acoustic waves,[13–15] or UV cross-linking,[18] to name a few. These existing approaches for creating living cell-based arrays rely on complicated surface modifications, require special equipment, or lack scalability, limiting their application on a broader scale.

We sought to develop a simple and efficient cell-patterning method for the implementation of functional biological screens, with the end goal of using this method to design a nano-liter scale neutralization assay to screen for neutralizing antibodies against HIV. This patterning method relies on a unique technique for patterning target cells into living cell arrays using mechanical disruption of a monolayer of target cells with a poly(dimethylsiloxane) (PDMS) array of subnanoliter wells (or nanowells).[17] We call this method nanowell-assisted cell patterning (NWAP) (Figure 1a). Briefly, (i) a monolayer of target cells is formed on a microscope slide that has been functionalized with a specific antibody to a target cell surface marker (eg., anti-CD4), (ii) the slide uniformly-coated with target cells is sealed against the nanowell device and (iii) the slide is removed and the target cells that are disrupted due to

Author Manuscript Author Manuscript Author Manuscript Author Manuscript

the physical pressure applied by the nanowell during incubation are washed away, leaving patterns of cells that correspond to the original positions of the nanowells. The resulting 2-D target cell patterns are 50 μm to 250 μm in width. A fluorescently-labeled antibody specific to the initial antibodies coated on the glass slide is included in the incubation medium while the array is sealed, allowing for the formation of fluorescent patterns to register the locations of all cognate cell patterns. Here, we chose to use GHOST cells, a standard cell-line used for microtitre-plate based HIV neutralization assays,[18] as target cells for optimizing cell patterning and to demonstrate the platform for a nanoliter-scale neutralization assay. Using a standard epifluoresence microscope, the number of cells per pattern, as well as the pattern area, can be enumerated (Figure 1b). Compared to previously reported patterning methods, this method offers a unique advantage as it allows for the monolayer of cells to remain in contact with the contents of a single nanoliter-sized well for a desired period of time, allowing for the creation of discrete and controllable microenvironments created by the nanowell device. Furthermore, due to the fluorescence-aided registration, resulting patterns of cells can be easily tracked over time after the nanowell device is removed.

Using this method, cell patterns of varying sizes have been formed as determined by device geometry (Figure 1b), ranging from 50μm to 250μm. Additional sizes and shapes could be easily implemented based on device design. Additionally, the number of cells per pattern can be modulated based on the initial loading density of target cells (Figure S1a), allowing for control over the distribution of target cells. We found that the method is spatially robust, resulting in the reproducible formation of cell patterns over an entire surface of the microscope slide (Supplemental Figure S1b), corresponding to ~80,000 patterns for a pattern size of 50μm. Taken together, these data show that we have developed a scalable and simple method for patterning target cells into living cell-based arrays.

One simple application of living cell arrays is tracking migration and proliferation of patterned cells over time. This key design feature is important for applications that require cell motility, cell proliferation, cell death or the accumulation of fluorescent reporter signal over time as assay signal readouts. For example, typical migration assays and wound healing assays rely on seeding monolayers of cells, scratching away a target area, then imaging the closing of the area over time.[19] These assays are low throughput, and rely on manual creation of each individual area void of cells, typically using a pipette tip to physically scrape away a section of cells. To this end, we first demonstrated that NWAP could be used to track the migration and proliferation of thousands of patterns of cells by imaging arrays of cell patterns over the course of 48 hours. Using a 250μm device design, we interrogated 3,328 single wells and corresponding cell patterns in parallel, drastically increasing the throughput over traditional migration assays. We found that under standard conditions, individual cell patterns were lost after 24 hours (Figure 2a) due to cell migration and proliferation, and that patterned cells remained viable through at least 48 hrs.

The loss of cell patterns, although useful for migration assays, could limit the implementation of assays that require longer time scales, such as detection of viral infection. We tested the effect of several media additives and hydrogels to aid maintenance of the patterns. The addition of hydrogels, such as alginate and pluronic acid, as cell encapsulation materials, did not allow for maintenance of viable cells in cognate patterns (data not shown).

Author Manuscript Author Manuscript Author Manuscript Author Manuscript

We instead sought to determine if the addition of a focal adhesion kinase inhibitor (FAK) (PF573228) or Rho-kinase inhibitor (Y-27632), both shown to inhibit cell motility but not adhesion,[20] would allow for pattern maintenance. The addition of 10μM FAK inhibitor resulted in individual pattern maintenance over 48 hours (Figure S2) by lowering both the proliferation (Figure 2b) and migration (Figure 2c) of attached cells. These data show that the addition of FAK inhibitor allows for the tight coupling of nanowell and cognate cell pattern, which extends the options for signal readout that can be used for the design of cell-based screens in this format.

A significant advantage afforded by NWAP is the ability to directly link stimuli present in nanowells upon formation of the initial cell pattern with delayed signal development in target cells. To this end, we designed a high-throughput cell-based screen to rapidly identify neutralizing antibodies based on function. This assay requires that antibody secreting cells be loaded into the nanowell arrays, brought into contact with virus and target cells, and the percent infection determined after read-out of accumulation of fluorescent reporter in target cells (~48 hrs post-infection), where infectivity is determined by counting individual infected cells (Figure 3a). The coordination of several biological events was needed for the development of this assay, thus many key aspects were developed and characterized, including a controllable target cell patterning method, quantification of the kinetics of antibody secretion and viral infectivity, and the degree to which cell patterns were maintained during infection signal development.

Given that we could maintain patterns, and hence spatial registration of cognate patterns for the time required for fluorescence to accumulate in typical reporter cell lines, we sought to measure the infectivity of HIV pseudovirus in nanowells to determine if infection rates were affected by the assay format. GHOST cells produce green fluorescent protein (gfp) when infected with HIV, thus providing a fluorescent signal for the quantification of infection. We produced pseudovirus according to a previously described protocol [21] followed by volume concentration to reach high titers and determined their infectivity by flow cytometry (Figure S3). We found that virions were highly infective, with an average infectivity rate of ~55%. For all virus experiments using nanowells, virus preparations from the same day and batch were used for a given experiment. To demonstrate infection of target cells could be detected using NWAP, we loaded the nanowell array with virus and allowed infection to proceed for 3 hours at 37°C after sealing the array. The median percent infection of patterned target cells was 30% (Figure 3b). Additionally, the median percent infection did not vary significantly as a function of GHOST cell density (Figure S4). To characterize the kinetics of viral infection in the nanowells, virus was loaded onto the nanowell array, and arrays were sealed for 60, 120, 180, or 240 minutes (Figure 3c). Kinetic data for infection were fit as previously described,[22] and we found the $t_{1/2}$ of infection to be 126 minutes, consistent with previously reported values.[23] Taken together, these data indicated that virus was capable of infecting patterned target cells and the rate of infection was comparable to those previously reported in the literature.

To determine whether titers of antibody relevant to neutralization could be achieved using antibody-secreting cells in the nanowells, we determined the number of antibody secreting cells needed to produce the required amount of antibody given the size of each well. A

Author Manuscript Author Manuscript Author Manuscript Author Manuscript

Chinese hamster ovary (CHO) cell line producing the well-characterized neutralizing antibody b12 [1] was stained with calcein green and loaded onto the PDMS device, and microengraving was used to quantify antibody secretion to determine secretion rate as previously described (Figure S5).[24,25] Using the measured average secretion rate of 50 molecules per second per cell, we determined the concentration of antibody in each nanowell as a function of time (Supplemental Table 1). We found that a nanowell of 250 μm size containing one cell reached a concentration of 0.014 μg/mL in a time of three hours, close to the low range of reported IC_{50} values for b12 (0.04 to >20 μg/mL).[26–28]

To screen for neutralization of virus by neutralizing antibody secreting cells, we loaded the nanowells with cell lines secreting either the neutralizing antibody b12 or the non-neutralizing antibody b6. Cells were stained with viability dye and the arrays were imaged using an epifluoresence microscope in order to determine well occupancy. The nanowell device was then loaded with pseudovirus and sealed with target GHOST cells for 3 hours. In order to slow the viral entry process to ensure high titers of antibody were reached prior to infection, sub-nanomolar concentration of the small molecule TAK779 was added with the virus prior to loading onto the array (Supplemental Table 2), as previous studies have demonstrated that TAK779 lowers the effective CCR5 concentration and thus, slows HIV-1 entry.[29,30] After the incubation, the target cell slide was removed, washed, and placed in media containing FAK inhibitor for 48 hours in order to maintain spatial registration of cell patterns. We found that the relative infectivity in target patterns per nanowell decreased significantly as a function of the number of b12 secreting cells, but not b6 cells (Figure 4). Additionally, we found that as low as one b12 secreting cell per well led to a significant decrease in the infection rate of target cells ($p = 0.0307$). These data agree with our calculated antibody secretion rate and known IC50 range for b12, and show that we can detect neutralization by b12 as a decrease in percent infection of target GHOST cells using this assay format.

In order to assess the performance of this assay format for the classification of antibody secreting cells into those that produce neutralizing antibodies (neutralizers) versus those that do not produce neutralizing antibodies (non-neutralizers), we generated receiver operating characteristic (ROC) curves (Figure 5a).[31] These curves allow for the characterization of screen performance in terms of sensitivity (true positive rate) and specificity (true negative rate). We used data obtained from CHO cells secreting b12, a canonical neutralizing antibody against HIV, to determine proper thresholds for classifying antibody-secreting cells as a neutralizer based on the decrease in percent infection of patterned target cells as compared to patterned target cells whose cognate nanowell did not contain a b12 cell.

The goal of the screen is to identify neutralizers accurately while minimizing false positives; thus, we would aim to increase the positive predictive value (PPV) while also maintaining a high negative predictive value (NPV). Infectivity thresholds were calculated based on cell patterns originating from nanowells containing no antibody secreting cells (ie: only virus). We calculated the PPV and NPV for several thresholds of infection rate as shown given a variable prevalence of neutralizers (1%, 10%, or 50%) in a hypothetical population of antibody secreting cells being screened (Figure 5b). We found that our PPV was highest (27%) for a population prevalence of 10% neutralizers when the threshold for calling

Author Manuscript Author Manuscript Author Manuscript Author Manuscript

neutralizers was most stringent: median – 1SD (Figure 5b). This result would suggest that this screen would be well suited for screening libraries of antibody secreting cells, where oversampling the library by at least 4-fold would result in identification of all neutralizers present in the population.

Alternatively, increasing the prevalence of neutralizers to 50% of the population screened would lead to dramatic increases in PPV rate, which indicates that this screen would best be implemented on pre-enriched populations of antibody secreting cells. We also found that we could obtain higher true positive rates when neutralizers were determined from nanowells containing >5 b12 cells (Supplemental Table 3), which could indicate that higher antibody secretion rates would improve screening sensitivity. The addition of TAK779, the small molecule inhibitor or viral entry, to the virus prior to incubating with target cells drastically improved the sensitivity and specificity of the assay across all thresholds (Supplemental Table 3).

Finally, we performed the nano-neutralization assay with additional antibody-secreting cell lines producing the non-neutralizing antibody 4D20 and the gp41-directed neutralizing antibody 2F5 to determine if we could detect a decrease in infection against a background population of non-specific antibody secreting cells, as well as determine if we could detect neutralization against another viral epitope (i.e., gp41) (Figure 5a). ROC curves for all antibody secreting cell lines tested indicated that the screen allows for the identification of neutralizing, non-neutralizing and weakly neutralizing antibodies, where the true positive rates are higher for cell lines producing higher affinity neutralizing antibodies (i.e., b12). Based on the calculated area under the curve (AUC) values for each cell line, we can use the nano-neutralization assay to identify b12 neutralizers with 70.95% accuracy and 2F5 with 66.06% accuracy. Using 4D20 cells, which secrete a non-neutralizing antibody, we found the accuracy to be 50%, which is in agreement with the fact that we do not detect neutralization from this cell line (Figure S6). Interestingly, we found that the non-neutralizer b6 could also be classified with 63.67% accuracy. The ability of b6 to bind with weak affinity to gp120 [32] could have contributed to the increase above background compared to 4D20. Taken together with high PPV rates for b12, these data show that the nano-neutralization screen can identify neutralizing antibody secreting cells with a high specificity, with a bias towards identification of strongly neutralizing antibodies.

In conclusion, we have developed a versatile and scalable method for implementing high-throughput and functional cell-based screens. This method relies on a novel cell patterning technique, NWAP, that can be implemented to measure many cellular behaviors, including cell migration, proliferation, and infection; this approach can readily be extended to apoptosis, cell-cell interactions, or even activation of patterned cells. Using this method, we designed and implemented a functional nanoliter-scale neutralization assay for single-cell secreted neutralizing antibodies against HIV. This high-throughput approach allows for the interrogation of thousands of antibody secreting cells in parallel while leveraging miniaturization to reduce reagent use. A key advantage afforded by this method is the ability to spatially register each individual cell pattern with each cognate nanowell, allowing a link between the contents of each nanowell and the result on the cellular behavior within each pattern to be maintained. This attribute, coupled with its high-throughput and flexible nature,

Author Manuscript Author Manuscript Author Manuscript Author Manuscript

makes the assay a highly promising tool for the development of high-content screens to identify lead therapeutics based on function. Additionally, this process reduces reagent use and can be scaled to evaluate ~10^4 cells per assay in 3 days, which would require ~26 384-well microtitre plates by comparison. The features of this screen, including single-cell counting capability for infection, short incubation times, and no pre-incubation of virus and antibody suggest that it should facilitate the identification of strong neutralizing antibodies in screens. This assay can drastically reduce the time and resources required to discover antibodies with high therapeutic potential. Finally, the simplicity of this assay should also facilitate its implementation for identifying antibodies for other therapeutic applications, including ones with oncolytic function, effector function, or bi-specific binding abilities.

Experimental Section

Tissue culture

The following reagent was obtained through the AIDS Reagent Program, Division of AIDS, NIAID, NIH: Ghost(3)X4/R5 from Drs. Vineet N. KewalRamani and Dan R. Littman. GHOST cells were maintained in complete media (Dulbecco's Modified Eagle Medium (supplier) with 10% Fetal Bovine Serum (FBS), supplemented with 1% Penicillin/ Streptomycin, 500 μg/ml G418 (supplier), 100 μg/ml hygromycin (supplier), and 1 μg/ml puromycin (supplier)) and discarded after 15 passages. Chinese hamster ovary (CHO) cell lines producing b12 (anti-gp120), 2F5 (anti-gp41) or b6 antibodies (courtesy of D. Burton, Scripps Institute) were cultured in ProCHO-5 media (Lonza) with 10% FBS, 1× HT supplement (Gibco), 1× GS supplement (Sigma–Aldrich), 100 U/mL penicillin, 100 mg/mL streptomycin and 50mM l-methionine sulfoxime (Sigma–Aldrich). A human B cell hybridoma cell line producing the 4D20 (anti-hemagglutinin) antibody (courtesy of J. Crow, Vanderbilt University) was adapted to grow in HL-1 medial containing 15% (v/v) FBS, 2mM l-glutamine, and 1mM sodium hyruvate. Cultures were passaged every 3–5 days and using when 60–70% confluent. ROCK inhibitor (Y-27632) and FAK inhibitor (PF-573228) were purchased from Tocris Bioscience, and suspended according to the manufactures instructions. *Fabrication of nanowell arrays*: Arrays of nanowells with the indicated geometries were fabricated using photolithography and replica molding with poly(dimethylsiloxane) (Sylgard 184, Dow Corning).[24] Photoresist (SU-8, Microchem) was spun on a 4 inch-silicon wafer to achieve 50 μm thickness, and patterns were created using a transparency photomask (CAD/Art Services) to produce a master with a positive relief pattern of the array of nanowells. PDMS was cast onto the master, cured for 3 h at 60 °C, removed, and stored at ambient conditions until use. The array of nanowells was treated with an oxygen plasma (PDC-32G, Harrick Plasma) for 4 minutes immediately prior to use, then placed directly into 0.5% (v/w) Bovine Serum albumin (BSA) in Phosphate Buffered Saline (PBS).

Cell patterning

GHOST cells were washed in complete media and resuspended in serum-free DMEM (SF-DMEM) at 1.5 x 10^6 cells per 120 μl unless indicated otherwise. Poly-l-lysine slides were coated with 85 μl of 25 μg/ml mouse anti-human CD4 antibody diluted in borate buffer under a LifterSlip™ (EMS). The slides were blocked for 30 min in 3% (v/w) milk in PBS

Author Manuscript Author Manuscript Author Manuscript Author Manuscript

and washed twice for 5 min in PBS on a rocker. 120 μl of GHOST cell suspension was then added to each slide under a LifterSlip™ (EMS) and incubated for 15 min at room temperature (RT). The cell-coated slides were then incubated in complete GHOST cell media for 1 hr at 37°C for attachment to the surface. For patterning, 350 μl of 5 μg/ml fluorescently labeled goat anti-mouse IgG (H+L) (Invitrogen) diluted in SF-DMEM was then added to each nanowell device to cover the entire surface. The cell-coated slide was then brought in contact with the nanowell device to seal the wells, and the assembly was incubated for 2–3 hrs at 37°C. After removal, the cell-patterned slides were washed twice for 5 min in PBS to wash away disrupted cells. Before imaging, slides were fixed to a 4-well dish with 2% agarose (Difco Agar Noble, BD) at the four corners of the slide. For viability staining, 4 ml of 2 μM calcein violet AM (Invitrogen) diluted in PBS was added to each slide immediately prior to imaging.

Imaging and data analysis

The cell arrays were imaged with an epi-fluorescence microscope (Zeiss). The slides were aligned using the background channel and imaged in an automated fashion. The images were analyzed with a custom analysis software, which uses the background fluorescence channel to locate each element of the array within the image, identifies the cells that are fluorescent in any channel of interest, and returns the number of cells per array element, and their intensity, size, and position. [33]

Pseudovirus production

Pseudovirus was produced using transient transfection of HEK 293 cells as previously described, with modifications. [21] Briefly, HEK 293 cells were seeded into T25 tissue culture flasks and allowed to adhere overnight. The following morning, 5 μg each of pSG3Δenv and pYU2ΔCT plasmids was transfected into the cells using Genjet (Signagen, Rockville, MD) according to manufacturers protocol in serum free HL-1 media. After 48 hrs, media was collected and virus spun concentrated 10-fold using Amicon Ultra 100K centrifugal filter units (Millipore, Bellerica, MA) and stored at −80°C until use.

Microengraving

Microengraving to detect antibody titres secreted from CHO b12 cell line was performed as previously described. [24,25] Poly-l-lysine slides were coated with Zymax goat-anti-human (25 μg/mL, Life Technologies) capture antibody. Microengraving was allowed to proceed for three hours, after which, protein arrays were scanned on a GenePix 4200AL and analyzed in GenePix Pro 6.0 (Molecular Devices). Data analysis was performed as previously described. [34]

Virus Infectivity Assay

For assessing infectivity of produced virus, GHOST cells were seeded at 50,000 cells per well in a 24-well plate (BD Falcon) and allowed to adhere overnight. Serial dilutions of psuedovirus were added to each well the following day for infection. After three hours, cells were washed and placed back in the incubator. After 48 hours, cells were detached with trypsin, fixed with paraformaldehyde, and infection assayed by flow cytometry.

Author Manuscript Author Manuscript Author Manuscript Author Manuscript

Virus infection was also assessed using the nanowells. Nanowells were loaded with 500 μL of virus then sealed with a target cell-covered glass slide as described above. After 3 hrs, arrays were removed, washed 2x with PBS, and placed into culture media for 48 hrs. Cell-arrays were scanned as described above to determine the number of infected cells per pattern.

Cell migration inhibition assay

Cell patterns were formed as described above. Arrays were imaged at 0, 24, and 48 hrs immediately after addition of 1μM calcein AM live cell stain (Life Technologies) in PBS. Media additives were diluted directly into culture media at the indicated concentration. Cell proliferation (P) was calculated per block (4 wells per block) as the ratio of cells at time of imaging to the number of starting cells at time zero. Cell migration (M) was defined as the number of cells that migrated out of the pattern areas initially identified by the wells, and calculated as $N_{full}(48hrs) - N_{well}(48hrs)$, where N_{full} is the number of cells per field of view, and N_{well} is the total number of cells in all four patterns within the view.

Neutralization assay

Cell patterns were formed as described above with the following modifications. Antibody secreting cell lines were stained with 1μM CellTracker™ red and 1μM Sytox green (Life Technologies). Arrays were loaded to a density of 0 to10 cells per well, and bright field and fluorescence images were acquired with an automated epi-fluorescence microscope (Zeiss) equipped with an EM-CCD camera (ImagEM, Hamamatsu). The array containing antibody secreting cells was loaded with 400uL pseudovirus containing 4 μg/mL of goat-anti-mouse background stain (AlexaFluor 647), then brought into contact with a GHOST cell covered slide for 3 hrs. The GHOST cell covered slide was then removed, washed 2x with PBS, and placed into media for 24 hrs. At 24 hrs, media was replaced with fresh media containing 10 μM FAK inhibitor (PF-573228). Cell arrays were imaged at 48 hrs immediately after addition of 2 μM calcein violet AM and 3 μg/mL Hoechst nuclear stain.

Statistical Analysis

All statistical analyses were performed using Prism 6 (V 6.0e). Statistical tests used are indicated where appropriate.

Supplementary Material

Refer to Web version on PubMed Central for supplementary material.

Acknowledgments

This work was supported in part by the Bill & Melinda Gates Foundation, the International AIDS Vaccine Initiative Innovation award, the W.M. Keck Foundation and the NIH/NIAID (5 U19 A1090970). This work was also supported in part by the Koch Institute Support (core) Grant P30-CA14051 from the National Cancer Institute. The content is solely the responsibility of the authors and does not necessarily represent the official views of the International AIDS Vaccine Initiative, National Institute of Allergy And Infectious Diseases, or the National Institutes of Health. J.C.L. is a Camille Dreyfus Teacher-Scholar. The authors would like to thank Bin Jia for help with HIV psuedovirus production.

Author Manuscript Author Manuscript Author Manuscript Author Manuscript

References

1. van Gils MJ, Sanders RW. Virology. 2013; 435:46–56. [PubMed: 23217615]
2. Debs BE, Utharala R, Balyasnikova IV, Griffiths AD, Merten CA. PNAS. 2012:11570–11575. [PubMed: 22753519]
3. Walker LM, Phogat SK, Chan-Hui PY, Wagner D, Phung P, Goss JL, Wrin T, Simek MD, Fling S, Mitcham JL, Lehrman JK, Priddy FH, Olsen OA, Frey SM, Hammond PW, Kaminsky S, Zamb T, Moyle M, Koff WC, Poignard P, Burton DR. Science. 2009; 326:285–289. [PubMed: 19729618]
4. Fernandes TG, Diogo MM, Clark DS, Dordick JS, Cabral JMS. Protocol Principal Investigators G. Trends in Biotechnology. 2009; 27:342–349. [PubMed: 19398140]
5. Guo MT, Rotem A, Heyman JA, Weitz DA. Lab Chip. 2012; 12:2146. [PubMed: 22318506]
6. Baret JC, Beck Y, Billas-Massobrio I, Moras D, Griffiths AD. Chemistry & Biology. 2010; 17:528–536. [PubMed: 20534350]
7. Zang R, Li D, Tang I-C, Wang J, Yang S-T. International Journal of Biotechnology for Wellness Industries. 2012:31–51.
8. Flaim CJ, Chien S, Bhatia SN. Nat Meth. 2005; 2:119–125.
9. Albrecht DR, Tsang VL, Sah RL, Bhatia SN. Lab Chip. 2005; 5:111. [PubMed: 15616749]
10. Chen CS. Science. 1997; 276:1425–1428. [PubMed: 9162012]
11. Berg MC, Yang SY, Hammond PT, Rubner MF. Langmuir. 2004; 20:1362–1368. [PubMed: 15803720]
12. Takayama, Kotake Y, Haga N, Suzuki T, Mabuchi T. Kunihiko. 2011:1–4.
13. Ding X, Shi J, Lin SCS, Yazdi S, Kiraly B, Huang TJ. Lab Chip. 2012; 12:2491. [PubMed: 22648600]
14. Shi J, Ahmed D, Mao X, Lin SCS, Lawita A, Huang TJ. Lab Chip. 2009; 9:2890–2895. [PubMed: 19789740]
15. Guoa F, Lia P, French JB, Mao Z, Zhao H, Li S, Nama N, Fick JR, Benkovic SJ, Huang TJ. PNAS. 2015; 112:43–48. [PubMed: 25535339]
16. Fink J, Th ry M, Azioune A, Dupont R, Chatelain FO, Bornens M, Piel M. Lab Chip. 2007; 7:672. [PubMed: 17538708]
17. Love JC, Ronan JL, Grotenbreg GM, van der Veen AG, Ploegh HL. Nature Biotechnology. 2006; 24:703–707.
18. Morner A, Bjorndal A, Albert J, KewalRamani VN, Littman DR, Inoue R, Thornstensson R, Fenyo EM, Bjorling E. Journal of Virology. 1999:2343–2349. [PubMed: 9971817]
19. Rodriguez LG, Wu X, Guan JL. Methods in Molecular Biology. 2007; 294:23–29. [PubMed: 15576902]
20. Loerke D, le Duc Q, Blonk I, Kerstens A, Spanjaard E, Machacek M, Danuser G, de Rooij J. Science Signaling. 2012; 5:rs5–rs5. [PubMed: 22763340]
21. Montefiori, DC. HIV Protocols. 2. Prasad, VR.; Kalpana, GV., editors. 2009. p. 485
22. Platt EJ, Durnin JP, Kabat D. Journal of Virology. 2005; 79:4347–4356. [PubMed: 15767435]
23. Reeves JD, Gallo SA, Ahmad N, Miamidian JL, Harvey PE, Sharron M, Pohlmann S, Sfakianos JN, Derdeyn CA, Blumenthal R, Hunter E, Doms RW. PNAS. 2002; 99:16249–16254. [PubMed: 12444251]
24. Han Q, Bradshaw EM, Nilsson B, Hafler DA, Love JC. Lab Chip. 2010:10, 11, 1391–1400.
25. Ogunniyi AO, Thomas BA, Politano TJ, Varadarajan N, Landais E, Poignard P, Walker BD, Kwon DS, Love JC. Vaccine. 2014:32, 24, 2866–73.
26. Moldt B, Rakasz EG, Schultz N, Chan-Hui PY, Swiderek K, Weisgrau KL, Piaskowski SM, Bergman Z, Watkins DI, Poignard P, Burton DR. Proceedings of the National Academy of Sciences. 2012; 109:18921–18925.
27. Blish CA, Nguyen M-A, Overbaugh J. PLoS Medicine. 2008:1–14.
28. Burton DR, Pyati J, Koduri R, Sharp SJ, Thornton GB, Parren PWHI, Sawyer LSW, Lamacchia M, Garratty E, Stiehm ER, Bryson YJ, Cao Y, Moore JP, Ho DD, Barbas CF III. Science. 1994:1–4.
29. Baba M. PNAS. 1999:1–6.

Author Manuscript Author Manuscript Author Manuscript Author Manuscript

30. Platt EJ, Kozak SL, Durnin JP, Hope TJ, Kabat D. Journal of Virology. 2010; 84:3106–3110. [PubMed: 20042508]
31. Baker SG. Journal of the National Cancer Institute. 2003; 95:511–515. [PubMed: 12671018]
32. Pantophlet R, Ollmann Saphire E, Poignard P, Parren PWHI, Wilson IA, Burton DR. Journal of Virology. 2003; 77:642–658. [PubMed: 12477867]
33. Gierahn TM, Loginov D, Love JC. Journal of Proteome Research. 2014; 13:362–371. [PubMed: 24417579]
34. Ogunniyi AO, Story CM, Papa E, Guillen E, Love JC. Nature Protocols. 2009; 4:767–782. [PubMed: 19528952]

Author Manuscript Author Manuscript Author Manuscript Author Manuscript

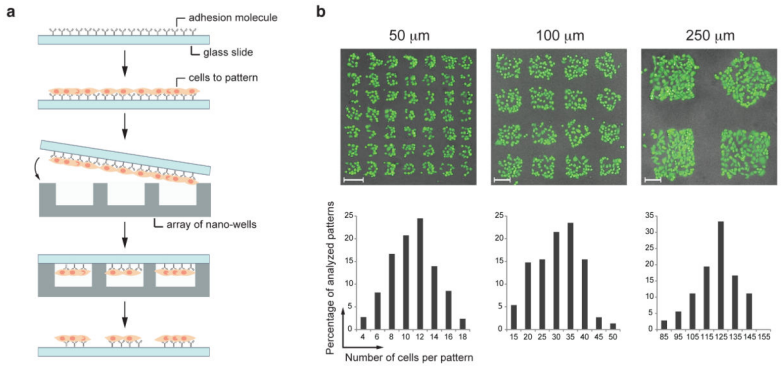

Figure 1.

Nanowell-assisted cell patterning (NWAP). **(a)** Patterning schematic shows the process for creating patterns using a nanowell device. **(b)** Patterns of different sizes were created by altering the design of the nanowell device used. Cells were stained with calcein green and the array was imaged using an epi-fluoresence microscope. The number of cells per pattern was then enumerated. Representative images from three designs are shown, along with histograms of the number of cells per cell island. Scale bar 50 μm.

Author Manuscript Author Manuscript Author Manuscript Author Manuscript

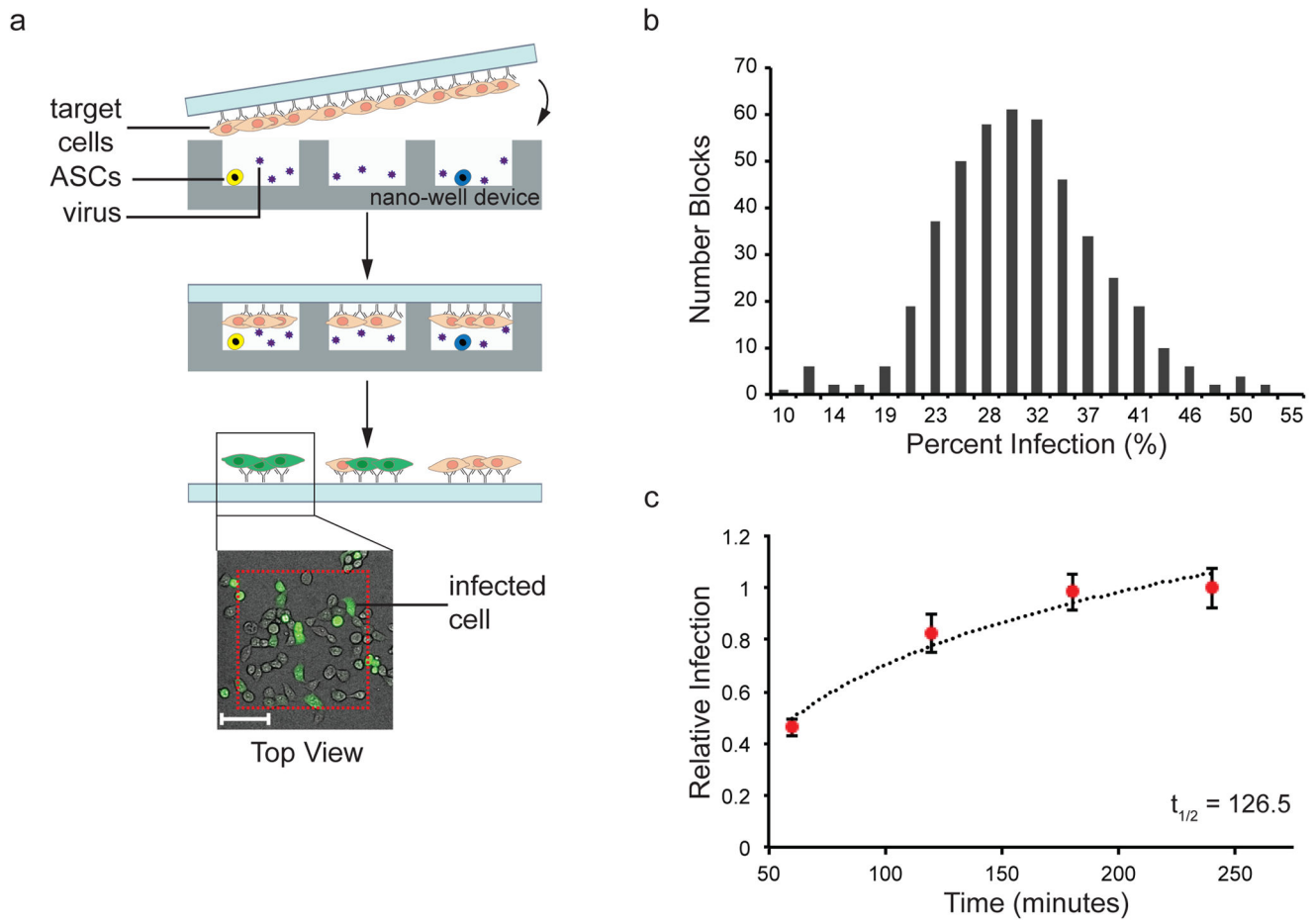

Figure 2.

The addition of a focal adhesion kinase (FAK) inhibitor (PF-573228) allowed for pattern maintenance over time. **A)** Representative images of cell patterns in the presence or absence of FAK inhibitor after 24 or 48 hours of growth. Cells were stained with calcein green before imaging. Background registration patterns are shown in purple. Scale bar 100 μm. **B)** Addition of FAK inhibitor reduced proliferation of patterned cells, where proliferation was calculated as the ratio of cells per block (N_t) divided by the initial cells per block (N_{to}). **C)** Addition of FAK inhibitor reduced migration of patterned cells. Migration was defined as the number of cells migrating out of patterns. **** $p < 0.0001$, Mann-Whitney U test.

Author Manuscript Author Manuscript Author Manuscript Author Manuscript

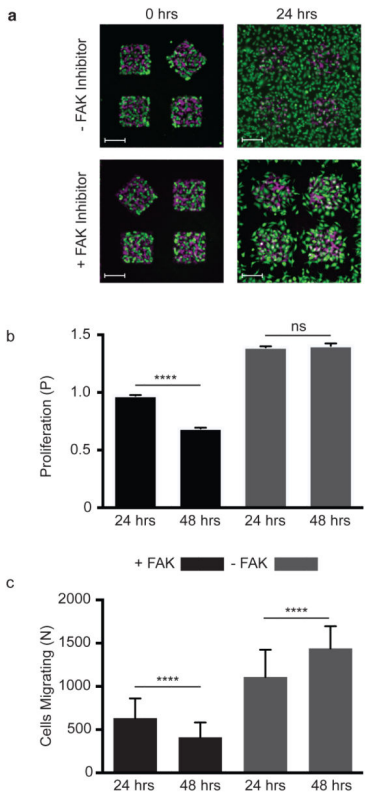

Figure 3.

Infection of target cells by HIV pseudovirus on glass (without FAK inhibitor). (a) *Top:* Schematic of nano-neutralization assay, showing: *i*. antibody secreting cells (ASCs) in nanowells, *ii*. incubation of target GHOST cells with ASCs and HIV virus to allow for neutralization, and *iii*. readout accomplished by enumerating infected (gfp^+) GHOST cells per pattern. *Bottom:* Representative image of infected GHOST cells (green) patterned on glass, where red dashed lines show the original locations of wells. Scale bar 100 μm. Assay schematic and sample image of infected cells on glass. Scale bar 100 μm. (b) Histogram of infectivity rate of cell patterns in the absence of neutralizing antibodies. Nanowell-assisted cell patterning was performed with 250 μm sized wells loaded with pseudovirus. (c) The kinetics of virus infection were determined by infecting GHOST cells for the indicated amount of time in the nanowells. Using the method of Platt *et al.*, the $t_{1/2}$ of infection was determined to be 123 minutes. Dotted line shows approximate best fit ($R^2 = 0.95524$): $y_{relinf} = 0.405\ln(t_{min})-1.163$. The mean and SEM for relative infectivity are plotted.

Author Manuscript Author Manuscript Author Manuscript Author Manuscript

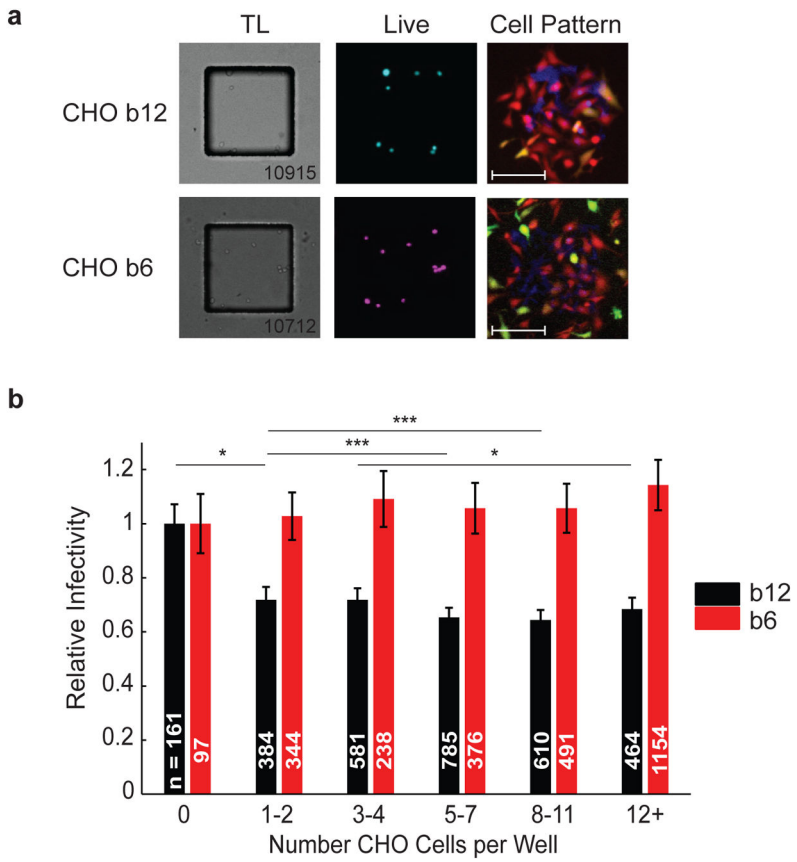

Figure 4.

Implementation of nano-neutralization assay using cell lines producing the neutralizing antibodies b12 or b6. **(a)** Sample images of nanowell array loaded with stained CHO b12 (cyan) or CHO b6 (pink) cells. For cell pattern images of target GHOST cells, live stain is red, infected cells are green, and the background of each pattern is blue. **(b)** Quantification of relative infectivity as a function of number of CHO b6 (red bars) or CHO b12 (black bars) per nanowell. The number of measured events is indicated on each bar, error bars were propagated from the SEM and indicated comparisons between black bars. ***, $p < 0.001$, *, $p < 0.05$, Kruskal-Wallis test with Dunn's multiple comparison post-test.

Author Manuscript Author Manuscript Author Manuscript Author Manuscript

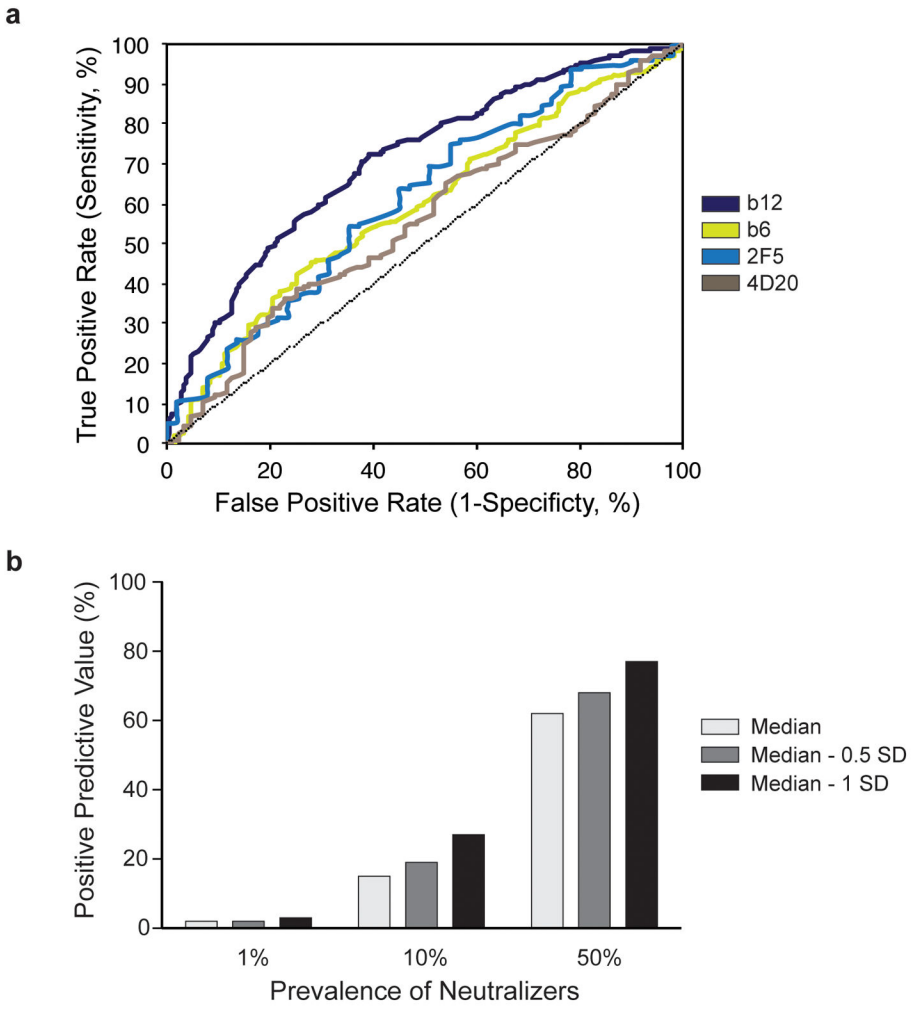

Figure 5.

ROC curve analysis of nano-neutralization assay. **(a)** ROC curves are shown for each antibody secreting cell line screened using the nano-neutralization assay. **(b)** Calculation of positive predictive value of b12 screen for indicated infectivity thresholds and neutralizer prevalence. Infectivity thresholds were determined from wells containing no antibody-secreting cells.